

# Preparations, X-ray Crystal Structures, EH Band Calculations, and Physical Properties of [(TTF)<sub>6</sub>(H)(XM<sub>12</sub>O<sub>40</sub>)(Et<sub>4</sub>N)] (M = W, Mo; X = P, Si): Evidence of Electron Transfer between Organic Donors and Polyoxometalates

L. Ouahab,\* M. Bencharif,<sup>†</sup> A. Mhanni, D. Pelloquin,<sup>‡</sup> J.-F. Halet,\* O. Peña, J. Padiou, and D. Grandjean

Laboratoire de Chimie du Solide et Inorganique Moléculaire, U.R.A. 254 CNRS, Université de Rennes I, 35042 Rennes Cedex, France.

C. Garrigou-Lagrange, J. Amiell, and P. Delhaes\*

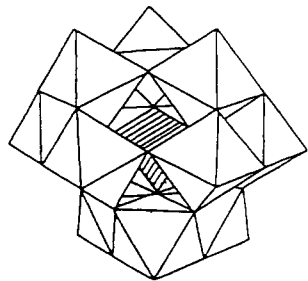
Centre de Recherche Paul Pascal, Avenue Albert Schweitzer, 33600 Pessac, France

Received December 18, 1991. Revised Manuscript Received February 14, 1992

The preparation, X-ray crystal structures, and conducting, optical, ESR, and magnetic properties of the (TTF)<sub>6</sub>(H)(XM<sub>12</sub>O<sub>40</sub>)(Et<sub>4</sub>N) salts are reported [1, X = P, M = W; 2, X = Si, M = W; 3, X = P, M = Mo; 4, X = Si, M = Mo]. The four compounds are isostructural and crystallize in the orthorhombic space group *Cmmm*. 1: *M<sub>r</sub>* = 4234.54; *a* = 15.563 (8), *b* = 19.497 (8), *c* = 14.178 (7) Å, *V* = 4302 Å<sup>3</sup>, *Z* = 2, *d<sub>calc</sub>* = 3.269 g cm<sup>-3</sup>, *R* = 0.040. 2: *M<sub>r</sub>* = 4231.65; *a* = 15.460 (8), *b* = 19.357 (5), *c* = 14.154 (3), *V* = 4235.7 Å<sup>3</sup>, *Z* = 2, *d<sub>calc</sub>* = 3.318 g cm<sup>-3</sup>, *R* = 0.069. 3: *M<sub>r</sub>* = 3179.6; *a* = 15.383 (2), *b* = 19.284 (5), *c* = 14.088 (9) Å, *V* = 4179.3 Å<sup>3</sup>, *Z* = 2, *d<sub>calc</sub>* = 2.527 g cm<sup>-3</sup>, *R* = 0.039. 4: *M<sub>r</sub>* = 3176.7; *a* = 15.455 (7) Å, *b* = 19.262 (8) Å, *c* = 14.089 (3) Å, *V* = 4194.3 Å<sup>3</sup>, *Z* = 2, *d<sub>calc</sub>* = 2.515 g cm<sup>-3</sup>, *R* = 0.050. Four out of the six TTF molecules form regular stacks with eclipsed overlaps, running along the [001] direction in channels formed by the inorganic [XM<sub>12</sub>O<sub>40</sub>] blocks and the two remaining isolated TTF. Magnetic susceptibility measurements indicate the presence of one unpaired electron per formula unit in the phosphometalate compounds (1 and 3), while the silicometalate compounds (2 and 4) exhibit a diamagnetic behavior. Accordingly, we observe ESR signal corresponding to W<sup>5+</sup> and Mo<sup>5+</sup> in the phosphometalate salts. The results obtained from physical measurements and band structure calculations suggest (TTF<sub>2</sub>)<sup>0</sup>(TTF<sub>4</sub>)<sup>2+</sup>(H)<sup>+</sup>(Et<sub>4</sub>N)<sup>+</sup>·(XM<sub>12</sub>O<sub>40</sub>)<sup>4-</sup> as being the appropriate formula for all of the four salts.

## Introduction

We are currently developing the solid-state chemistry and the physical properties of a new type of charge-transfer (CT) compounds.<sup>1-4</sup> These materials are made up of organic donors such as the tetrathiafulvalene (TTF) and inorganic acceptors derived from the polyoxometalates whose structures are made of the association of MO<sub>6</sub> (M = Mo, W, Nb) octahedra (I).<sup>5-7</sup>



I

Since the observation of a metallic state in the prototypical CT salt (TTF-TCNQ),<sup>8</sup> followed a few years later by the discovery of a superconducting state in the Bechgaard salts (TMTSF)<sub>2</sub>X, X = PF<sub>6</sub><sup>-</sup>, ClO<sub>4</sub><sup>-</sup>,<sup>9</sup> numerous works have been devoted to these one-dimensional organic materials. In another field, the polyoxometalates form a large class of compounds which attracts many research-

ers.<sup>10</sup> These polyanions present an interest because of their high electron-acceptor capabilities.<sup>11,12</sup> We focus our investigations on polyanions having the Lindquist<sup>13</sup> structure [(M<sub>6</sub>O<sub>19</sub>)<sup>n-</sup>] and the Keggin<sup>14</sup> structure [(XM<sub>12</sub>O<sub>40</sub>)<sup>n-</sup>, M = W, Mo; X = P, Si, Ge...].

- (1) Ouahab, L.; Bencharif, M.; Grandjean, D. *C. R. Acad. Sci. Paris* 1988, 307 II, 749.
- (2) (a) Triki, S.; Ouahab, L.; Padiou, J.; Grandjean, D. *J. Chem. Soc., Chem. Commun.* 1989, 1068. (b) Triki, S.; Ouahab, L.; Halet, J.-F.; Peña, O.; Padiou, J.; Grandjean, D.; Garrigou-Lagrange, C.; Delhaes, P. *J. Chem. Soc., Dalton Trans.*, in press.
- (3) Ouahab, L.; Triki, S.; Grandjean, D.; Bencharif, M.; Garrigou-Lagrange, C.; Delhaes, P. In *Lower-Dimensional Systems and Molecular Electronics*; Metzger, R. M., Day, P., Papavassillou, G. C., Eds.; Plenum Press: NATO ASI series, 1991; Vol. B248, p 185.
- (4) Mhanni, A.; Ouahab, L.; Peña, O.; Grandjean, D.; Garrigou-Lagrange, C.; Delhaes, P. *Synth. Met.* 1991, 41-43, 1703.
- (5) Souchay, P. *Ions Minéraux Condensés*; Masson: Paris, 1969.
- (6) Pope, M. T. In *Heteropoly and Isopoly Oxometalates*; Springer-Verlag: New York, 1983.
- (7) Evans, H. T., Jr. *Persp. Struct. Chem.* 1971, 4, 1.
- (8) (a) Ferraris, J.; Cowan, D. O.; Walatka, V.; Perlstein, J. H. *J. Am. Chem. Soc.* 1973, 95, 498. (b) Coleman, L. B.; Cohen, M. J.; Sandman, D. J.; Yamagishi, F. G.; Garito, A. F.; Heeger, A. J. *Solid State Commun.* 1973, 12, 1125.
- (9) (a) Bechgaard, K.; Jacobsen, S.; Mortensen, K.; Pedersen, H. J.; Thorup, N. *Solid. State Commun.* 1980, 33, 1119. (b) Jérôme, D.; Mazaud, A.; Ribault, M.; Bechgaard, K. *J. Phys. Lett.* 1980, 41, L95.
- (10) Pope, M. T.; Müller, A. *Angew. Chem., Int. Ed. Engl.* 1991, 30, 34.
- (11) Launay, J. P. *J. Inorg. Nucl. Chem.* 1976, 18, 807.
- (12) (a) Pope, M. T.; Varga, G. M. *Inorg. Chem.* 1966, 5, 1249. (b) Pope, M. T.; Papaconstantinou, E. *Ibid.* 1967, 6, 1147. (c) Varga, G. M.; Papaconstantinou, E.; Pope, M. T. *Ibid.* 1970, 9, 662. (d) Hill, C. L.; Bouchard, D. A.; Kadkhodayan, M.; Williamson, M. M.; Schmidt, J. A.; Hilinsky, E. F. *J. Am. Chem. Soc.* 1988, 110, 5471 and references therein.
- (13) Lindquist, I. *Ark. Kem.* 1953, 5, 247.
- (14) Keggin, J. F. *Proc. R. Soc. London, Ser. A* 1934, 144, 75.

\* To whom correspondence should be addressed.

<sup>†</sup> Post-graduate student of the Institut de Chimie, Université de Constantine, Algérie.

<sup>‡</sup> Undergraduate student of "Magistère Matériaux" Université de Rennes 1.

Table I. Crystal and Refinement Data for Compounds 1-4

	1	2	3	4
formula wt	4234.54	4231.65	3179.6	3176.7
cryst syst	orthorhombic	orthorhombic	orthorhombic	orthorhombic
space gp	<i>Cmmm</i>	<i>Cmmm</i>	<i>Cmmm</i>	<i>Cmmm</i>
a, Å	15.563 (8)	15.460 (4)	15.383 (2)	15.455 (7)
b, Å	19.497 (8)	19.357 (5)	19.284 (5)	19.262 (8)
c, Å	14.178 (7)	14.154 (3)	14.088 (9)	14.089 (3)
V, Å <sup>3</sup>	4302	4235.7	4179.3	4194.3
Z	2	2	2	2
d <sub>exp</sub> , g cm <sup>-3</sup>	3.23	3.22	2.51	2.49
d <sub>calc</sub> , g cm <sup>-3</sup>	3.269	3.318	2.527	2.515
diffractometer	Nonius CAD4	Nonius CAD4	Nonius CAD4	Nonius CAD4
radiation	Mo Kα	Mo Kα	Mo Kα	Mo Kα
wavelength, Å	0.710 73	0.710 73	0.710 73	0.710 73
scan method	θ-2θ	θ-2θ	θ-2θ	θ-2θ
cryst size, mm	0.2 × 0.1 × 0.08	0.15 × 0.1 × 0.1	0.25 × 0.1 × 0.15	0.15 × 0.1 × 0.1
μ(Mo Kα), cm <sup>-1</sup>	169.84	172.45	23.78	23.64
h,k,l range	0,18/0,23/±16	0,18/0,22/0,16	0,18/0,22/0,16	0,18/±22/0,16
2θ limits, deg	2-50	2-50	2-50	2-50
no. of rflns				
unique	1700	1544	1616	1522
I ≥ nσ(I)	1273, n = 3	1166, n = 6	1312, n = 6	1087, n = 3
R <sub>int</sub>	0.040			0.049
trans factors min, max	0.78, 1.32	0.73, 1.63	0.79, 1.32	0.882, 1.223
no. of variables	159	156	171	171
R(F), <sup>a</sup> R <sub>w</sub> (F) <sup>b</sup>	0.044, 0.088	0.069, 0.126	0.039, 0.060	0.050, 0.065
GOF <sup>c</sup>	0.904	1.587	1.595	1.443
Δ/σ	0.45	0.09	0.01	0.12
Δρ, e Å <sup>-3</sup>	1.05	1.745	0.674	1.048

<sup>a</sup>  $R = \sum [|F_o| - |F_c|] / \sum |F_o|$ . <sup>b</sup>  $R_w = [\sum w(|F_o| - |F_c|)^2 / \sum w|F_o|^2]^{1/2}$ .  $w = 4F_o^2 / [\sigma^2(I) - (0.07|F_o|^2)^2]$ . <sup>c</sup> Goodness of fit (GOF) =  $[\sum w(|F_o| - |F_c|)^2 / (N_{obs} - N_{var})]^{1/2}$ .

The combination of such large inorganic acceptor polyanions with organic substrates can increase the electronic dimensionality of these types of compounds from 0- to 3-D and offers the possibility of making materials where both organic donor and inorganic acceptor blocks are in a mixed-valence state. The stabilization of such a mixed-valence state is one of the most important prerequisites for the possible observation of conducting or magnetic properties according to electron delocalization along the organic systems or electron localization on the transition-metal centers of the inorganic counterpart.

This paper deals with the preparation and the characterizations of the first materials obtained from the reaction of TTF with some Keggin polyoxometalate salts.<sup>1,3,4</sup>

### Experimental Section

**Preparation.** TTF (Fluka) was used as received. Acetonitrile, dichloromethane, and dimethylformamide (Fluka) were distilled and passed through activated neutral alumina before use. The tetraethylammonium (Et<sub>4</sub>N) salts of the anions were prepared and recrystallized according to ref 15. Their stoichiometries were determined by elemental analysis. The electrocrystallizations were carried out in 25 cm<sup>3</sup> U-shaped cell with the two electrolytic compartments separated by a glass frit (porosity 3). The electrodes are 1-mm-diameter platinum wire and were immersed in the degassed solution to a depth of 2.5 cm. The densities were measured by floating in Clerici solution (see Table I).

(TTF)<sub>6</sub>(H)PW<sub>12</sub>O<sub>40</sub>(Et<sub>4</sub>N) (1) and (TTF)<sub>6</sub>(H)SiW<sub>12</sub>O<sub>40</sub>(Et<sub>4</sub>N) (2):<sup>15</sup> The anodic oxidation of the organic donor (TTF, 2 × 10<sup>-3</sup> M) under low constant current (I = 1 μA) in the presence of the tetraethylammonium salt of the XW<sub>12</sub>O<sub>40</sub> anions (10<sup>-2</sup> M) as

supporting electrolyte in acetonitrile leads to polyhedral block-shaped black crystals after 1 week. The stoichiometries were determined by X-ray crystal structure analysis and elemental analysis: Anal. Calcd (obsd) for 1, C<sub>44</sub>H<sub>45</sub>NO<sub>46</sub>PS<sub>24</sub>W<sub>12</sub>: C, 12.47 (12.45); H, 1.06 (1.02); N, 0.33 (0.35); S, 18.17 (17.49); P, 0.73 (0.75); W, 52.10 (52.90). Anal. Calcd (obsd) for 2, C<sub>44</sub>H<sub>45</sub>NO<sub>46</sub>SiS<sub>24</sub>W<sub>12</sub>: C, 12.48 (12.58); H, 1.06 (0.93); N, 0.33 (0.35); S, 18.18 (17.69); Si, 0.66, (0.70); W, 52.13, (52.06).

(TTF)<sub>6</sub>(H)PMo<sub>12</sub>O<sub>40</sub>(Et<sub>4</sub>N) (3) and (TTF)<sub>6</sub>(H)SiMo<sub>12</sub>O<sub>40</sub>(Et<sub>4</sub>N) (4): These compounds are obtained following the same method used for the tungstate anions with nevertheless small modifications. When acetonitrile solutions of TTF and (Et<sub>4</sub>N)XMo<sub>12</sub>O<sub>40</sub> are mixed, an instantaneous precipitate appears following redox reactions between highly oxidized (TTF) and highly reduced species [(Et<sub>4</sub>N)<sub>n</sub>XMo<sub>12</sub>O<sub>40</sub>; (X = P, n = 3) and (X = Si, n = 4)]. After 30 min, 10 mg of TTF is added again to the resulting dark solutions. The electrochemical cells are then connected. Polyhedral block-shaped black crystals are obtained after 1 week. The stoichiometries were determined by X-ray crystal structures and elemental analysis: Anal. Calcd (obsd) for 3, C<sub>44</sub>H<sub>45</sub>NO<sub>46</sub>PS<sub>24</sub>Mo<sub>12</sub>: C, 16.61 (16.88); H, 1.41 (1.23); N, 0.44 (0.45); S, 24.20 (23.65); P, 0.97 (0.99); Mo, 36.21 (36.67). Anal. Calcd (obsd) for 4, C<sub>44</sub>H<sub>45</sub>NO<sub>46</sub>SiS<sub>24</sub>Mo<sub>12</sub>: C, 16.62 (16.77); H, 1.41 (1.43); N, 0.44 (0.50); S, 24.22 (23.02); Si, 0.88 (1.18); Mo, 36.24 (36.34).

**X-ray Crystal Structure Analysis.** Black crystals of the title compounds were mounted on an Enraf-Nonius CAD4 diffractometer equipped with graphite crystal monochromatized Mo Kα radiation (λ = 0.710 73 Å). The intensities were collected by θ-2θ scans. Three standard reflections were measured every hour and revealed no fluctuations in intensities. One set of reflections was collected up to 2θ = 50°. The Lorentz, polarization, and absorption corrections were applied. The absorption corrections were performed using the DIFABS procedure.<sup>16</sup> The cell parameters, the *mmm* Laue symmetry, and the C-type lattice (*hkl*: *h* + *k* = 2*n* + 1) were determined by the Weissenberg and precession photograph methods. The cell dimensions have been refined by using the least-squares method from setting angles of 25 centered reflections. Among the three possible orthorhombic space groups, i.e., *C222*, *Cmm2* and *Cmmm*, corresponding to the extinction

(15) (a) The (Et<sub>4</sub>N)<sub>3</sub>(PW<sub>12</sub>O<sub>40</sub>), (Et<sub>4</sub>N)<sub>4</sub>(SiW<sub>12</sub>O<sub>40</sub>), and (Et<sub>4</sub>N)<sub>4</sub>(SiMo<sub>12</sub>O<sub>40</sub>) salts have been obtained by precipitation of the corresponding commercial acid with tetraethylammonium bromide in aqueous solution. The (Et<sub>4</sub>N)<sub>3</sub>(PMo<sub>12</sub>O<sub>40</sub>) salt has been prepared according to ref 38b. (b) In a first note (see ref 1), we unfortunately reported salt 1 as (TTF)<sub>6</sub>(XMo<sub>12</sub>O<sub>40</sub>)(Et<sub>4</sub>N)<sub>2</sub>. From the present investigations, we conclude unambiguously that this salt contains only one Et<sub>4</sub>N<sup>+</sup> unit.

(16) Walker, N.; Stuart, D. *Acta Crystallogr.* 1983, A39, 158.

Table II. Atomic Coordinates and Equivalent Isotropic Thermal Parameters for 1-4<sup>a</sup>

atom	x	y	z	B <sub>eq</sub> , Å <sup>2</sup>	atom	x	y	z	B <sub>eq</sub> , Å <sup>2</sup>
(a) (TTF) <sub>6</sub> HPW <sub>12</sub> O <sub>40</sub> [(C <sub>2</sub> H <sub>5</sub> ) <sub>4</sub> N] (1)					(c) (TTF) <sub>6</sub> HPMo <sub>12</sub> O <sub>40</sub> [(C <sub>2</sub> H <sub>5</sub> ) <sub>4</sub> N] (3)				
W1	-0.15933 (4)	0.000	0.18094 (6)	3.42 (1)	Mo1	-0.15805 (6)	0.000	0.18439 (7)	2.67 (2)
W2	-0.16462 (4)	-0.12678 (4)	0.000	3.28 (1)	Mo2	-0.16831 (6)	-0.12563 (5)	0.000	2.67 (2)
W3	0.000	-0.13127 (4)	0.17467 (6)	3.62 (1)	Mo3	0.000	-0.13388 (5)	0.17298 (8)	2.84 (2)
P	0.000	0.000	0.000	1.9 (2)	P	0.000	0.000	0.000	1.6 (1)
O1	-0.2330 (9)	0.000	0.266 (1)	6.6 (4)	O1	-0.2352 (6)	0.000	0.2657 (7)	5.4 (3)
O2	-0.2014 (6)	-0.0661 (5)	0.0923 (7)	6.0 (2)	O2	-0.2054 (5)	-0.0670 (4)	0.0948 (5)	6.1 (2)
O3	-0.2457 (9)	-0.1834 (7)	0.000	6.7 (4)	O3	-0.2489 (6)	-0.1814 (4)	0.000	5.9 (3)
O4	-0.0844 (6)	-0.1624 (6)	-0.0904 (7)	7.1 (3)	O4	-0.0875 (4)	-0.1655 (4)	-0.0920 (5)	5.5 (2)
O5	0.000	-0.1920 (9)	0.258 (1)	6.9 (4)	O5	0.000	-0.1944 (5)	0.2583 (6)	4.4 (2)
O6	-0.0818 (6)	-0.0677 (5)	0.2210 (9)	6.8 (3)	O6	-0.0829 (5)	-0.0702 (4)	0.2252 (6)	6.3 (2)
O7	-0.0551 (8)	-0.0460 (6)	0.061 (1)	2.4 (3)	O7	-0.0569 (5)	-0.0464 (5)	0.0640 (7)	7.5 (2)
TTF-A					TTF-A				
C1	0.500	-0.034 (1)	0.124 (1)	4.4 (4)	C1	0.500	-0.0341 (7)	0.1278 (8)	3.6 (3)
C2	0.542 (1)	-0.1622 (9)	0.116 (1)	6.8 (4)	C2	0.5445 (7)	-0.1629 (6)	0.1188 (8)	6.4 (3)
S1	0.5933 (2)	-0.0831 (3)	0.1222 (3)	6.0 (1)	S1	0.5944 (2)	-0.0834 (2)	0.1237 (2)	4.68 (6)
TTF-B					TTF-B				
C3	0.4549 (9)	0.1640 (8)	0.375 (1)	5.7 (4)	C3	0.4564 (6)	0.1630 (5)	0.3727 (7)	4.4 (2)
C4	0.500	0.034 (1)	0.378 (1)	4.5 (4)	C4	0.500	0.0354 (6)	0.3729 (7)	2.5 (2)
S2	0.4054 (2)	0.0828 (2)	0.3737 (3)	4.75 (8)	S2	0.4050 (1)	0.0835 (1)	0.3746 (2)	3.54 (5)
TTF-C					TTF-C				
C5	0.250	0.250	0.454 (1)	3.2 (3)	C5	0.25	0.25	0.4514 (8)	3.0 (2)
C6	0.2658 (9)	0.283 (1)	0.277 (1)	7.2 (5)	C6	0.2663 (6)	0.2813 (6)	0.2738 (7)	5.0 (2)
S3	0.2842 (2)	0.3203 (2)	0.3861 (3)	5.23 (9)	S3	0.2861 (2)	0.3206 (1)	0.3840 (2)	4.06 (5)
N	0.000	0.000	0.500	5.3 (8)*	N	0.000	0.000	0.500	3.3 (4)
C7	0.077 (3)	0.000	0.438 (4)	6 (1)*	C7	0.076 (2)	0.000	0.437 (2)	12.6 (9)
C8	0.165 (4)	0.000	0.500	4 (1)*	C8	0.166 (1)	0.000	0.500	4.6 (5)
C9	0.000	-0.067 (2)	0.438 (4)	6 (1)*	C9	0.000	-0.068 (1)	0.439 (2)	12.1 (8)
C10	0.000	-0.133 (3)	0.500	4 (1)*	C10	0.000	-0.138 (1)	0.500	6.4 (6)
(b) (TTF) <sub>6</sub> HSiW <sub>12</sub> O <sub>40</sub> (C <sub>2</sub> H <sub>5</sub> ) <sub>4</sub> N (2)					(d) (TTF) <sub>6</sub> HSiMo <sub>12</sub> O <sub>40</sub> [(C <sub>2</sub> H <sub>5</sub> ) <sub>4</sub> N] (4)				
W1	-0.15770 (7)	0.000	0.18041 (9)	2.93 (2)	Mo1	-0.1535 (1)	0.000	0.1850 (1)	3.52 (3)
W2	-0.16413 (6)	-0.12613 (6)	0.000	2.89 (2)	Mo2	-0.16890 (9)	-0.12261 (7)	0.000	3.58 (3)
W3	0.000	-0.13145 (6)	0.17269 (9)	3.00 (2)	Mo3	0.000	-0.13474 (7)	-0.1678 (1)	3.68 (3)
Si	0.000	0.000	0.000	2.6 (3)	Si1	0.000	0.000	0.000	2.2 (2)
O1	-0.235 (1)	0.000	0.262 (2)	5.2 (6)	O1	-0.2312 (9)	0.000	0.2654 (9)	6.0 (4)
O2	-0.2044 (9)	-0.0654 (8)	0.095 (1)	6.0 (4)	O2	-0.2062 (6)	-0.0667 (5)	0.0952 (6)	7.2 (2)
O3	-0.247 (1)	-0.181 (1)	0.000	5.5 (6)	O3	-0.25	-0.1797 (6)	0.000	6.3 (3)
O4	-0.085 (1)	-0.1657 (9)	-0.091 (1)	6.1 (4)	O4	-0.0886 (6)	-0.1670 (5)	-0.0918 (7)	6.9 (3)
O5	0.000	-0.192 (1)	0.257 (2)	4.7 (5)	O5	0.000	-0.1937 (6)	-0.2520 (9)	5.3 (3)
O6	-0.082 (1)	-0.0693 (8)	0.224 (1)	6.4 (4)	O6	0.0821 (6)	-0.0699 (6)	-0.2265 (7)	7.8 (3)
O7	-0.058 (1)	-0.050 (1)	0.066 (2)	2.2 (5)	O7	-0.0633 (7)	-0.0482 (6)	0.0662 (8)	7.7 (3)
TTF-A					TTF-A				
C1	0.500	-0.034 (1)	0.128 (2)	2.9 (6)	C1	0.500	-0.0353 (9)	0.1275 (9)	3.6 (4)
C2	0.541 (2)	-0.162 (1)	0.121 (2)	5.5 (6)	C2	0.546 (1)	-0.1629 (9)	0.119 (1)	8.6 (5)
S1	0.5936 (3)	-0.0839 (4)	0.1243 (5)	4.7 (1)	S1	0.5940 (2)	-0.0830 (2)	0.1239 (3)	5.65 (9)
TTF-B					TTF-B				
C3	0.458 (1)	0.166 (1)	0.369 (2)	5.1 (6)	C3	0.4572 (8)	0.1632 (7)	0.374 (1)	5.3 (3)
C4	0.500	0.034 (1)	0.374 (2)	2.8 (5)*	C4	0.500	0.0358 (8)	0.373 (1)	2.8 (3)
S2	0.4053 (3)	0.0833 (3)	0.3740 (4)	3.7 (1)	S2	0.4053 (2)	0.0836 (2)	0.3746 (2)	4.17 (7)
TTF-C					TTF-C				
C5	0.250	0.250	0.454 (2)	2.4 (5)	C5	0.25	0.25	0.452 (1)	3.1 (3)
C6	0.268 (1)	0.283 (2)	0.274 (2)	5.9 (7)	C6	0.2664 (8)	0.2821 (8)	0.2743 (9)	5.5 (4)
S3	0.2841 (4)	0.3210 (3)	0.3850 (5)	4.4 (1)	S3	0.2856 (2)	0.3209 (2)	0.3838 (3)	4.67 (8)
N	0.000	0.000	0.500	2.9 (9)*	N	0.000	0.000	0.500	3.2 (6)
C7	0.071 (4)	0.000	0.439 (6)	5 (2)*	C7	0.081 (2)	0.000	0.439 (3)	17 (2)
C8	0.163 (4)	0.000	0.500	3 (1)*	C8	0.166 (2)	0.000	0.500	5.9 (8)
C9	0.000	-0.062 (4)	0.427 (6)	6 (2)*	C9	0.000	-0.070 (3)	0.435 (3)	19 (2)
C10	0.000	-0.131 (4)	0.500	2 (1)*	C10	0.000	-0.139 (1)	0.500	10 (1)

<sup>a</sup> Starred atoms were refined isotropically.

conditions, the latter was retained on the basis of the successful solution and refinement of the structures. The crystal data are summarized in Table I.

The structure of 1 was solved by direct methods<sup>17</sup> and successive Fourier difference synthesis. The structure was refined by weighted anisotropic full-matrix least-squares methods. After refinement of positional and anisotropic ( $\beta_{ij}$ ) thermal parameters

for all non-hydrogen atoms, the positions of the H atoms were calculated [ $d(C-H) = 1.0$  Å;  $B_{eq} = 4.0$  Å<sup>2</sup>] and included as a fixed contribution to  $F_c$ . The other structures were refined by weighted anisotropic full-matrix least-squares methods on the basis of the structure solution of compound 1. Scattering factors and corrections for anomalous dispersion were taken from ref 18. The molecular and crystal structure illustrations were drawn with ORTEP.<sup>19</sup> All the calculations were performed on a PDP11/60 and a MicroVax 3100 computers using the SDP programs de-

(17) Main, P.; Fiske, S. J.; Hull, S. E.; Lessinger, L.; Germain, G.; Declercq, J. P.; Woolfson, M. M. MULTAN 84, A system of computer programs for the automatic solution of crystal structures from X-ray diffraction data; Universities of York (England) and Louvain (Belgium), 1984.

(18) International Table for X-ray Crystallography; Kynoch Press: Birmingham, 1974; Vol. IV; present distributor D. Reidel: Dordrecht.  
(19) Johnson, C. K. ORTEP, Report ORNL-3794; Oak Ridge National Laboratory, Oak Ridge, TN, 1965.

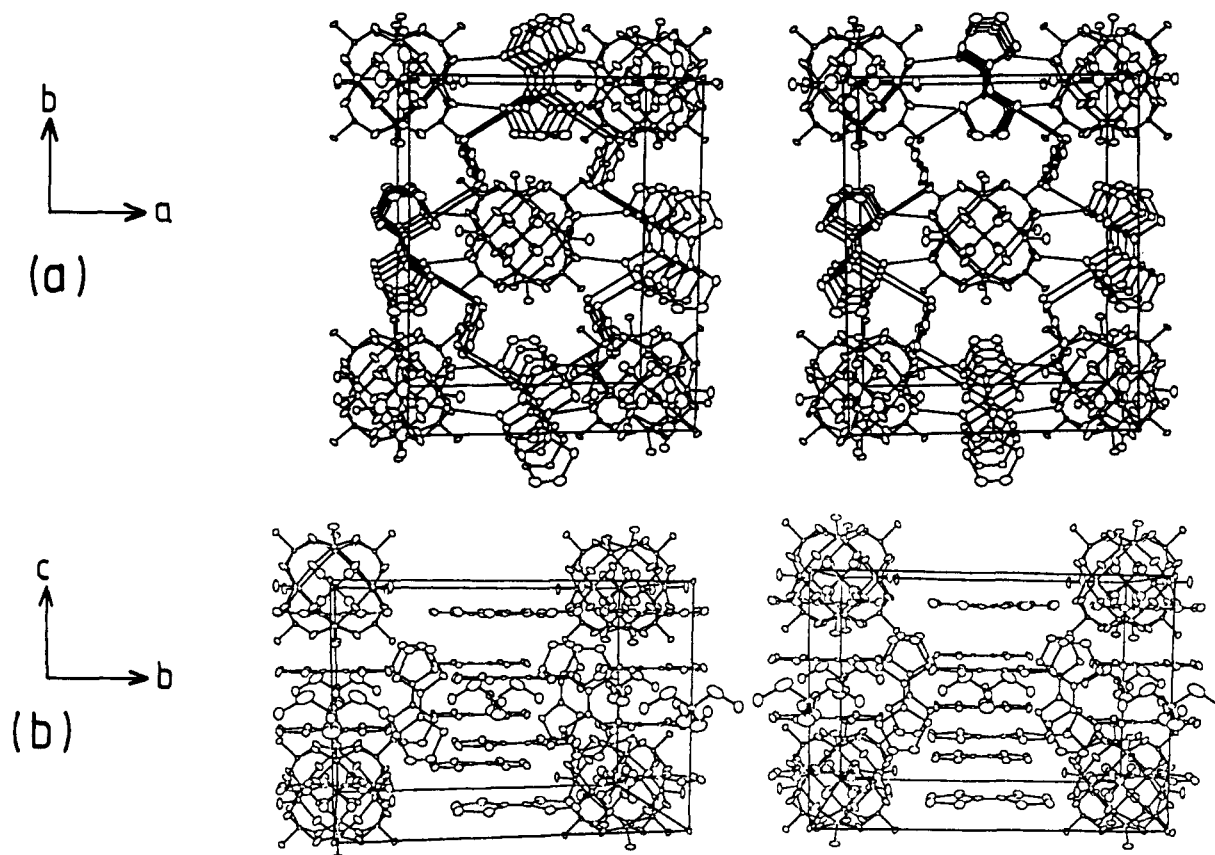


Figure 1. Stereoscopic views of the structure looking down the  $c$  and  $a$  directions showing the constituent units, the TTF stackings, and the eclipsed inter-TTF overlaps. Some  $\text{XM}_{12}\text{O}_{40}$  units are omitted for clarity.

scribed by Frenz.<sup>20</sup> The atomic coordinates are given in Table II.

**Electrical Conductivity.** The single-crystal room-temperature dc electrical conductivities measured by standard four-probe technique are ( $\sigma_{300\text{K}}$ ) =  $3 \times 10^{-2}$ ,  $5 \times 10^{-4}$ ,  $5 \times 10^{-2}$ , and  $10^{-4} \Omega^{-1} \text{cm}^{-1}$  for 1, 2, 3, and 4, respectively. Large current fluctuations were observed during our attempts to the measurements of the conductivity versus temperature. But in every case a semiconducting behavior has been detected.

**Spectroscopic Characterizations.** An IR Nicolet MX1 interferometer ( $350\text{--}4800 \text{ cm}^{-1}$ ) and a UV-vis Perkin-Elmer 350 spectrometer ( $3850\text{--}25000 \text{ cm}^{-1}$ ) were used for comparative transmission measurements of finely ground KBr pellet samples. The IR spectra were recorded at different temperatures down to 15 K with a  $^4\text{He}$  cryostat. An X-band Varian spectrometer equipped with an Oxford variable-temperature accessory was used for ESR experiments on single crystal. The results are presented in Figures 5–7.

**Magnetic Measurements.** Magnetic susceptibility measurements were performed on crystals using a SQUID susceptometer (SHE-VTS 906) between room temperature and 5 K. Susceptibility was corrected for diamagnetic contributions of anions, organic molecules, and tetraethylammonium group ( $\chi_{\text{DIA}} \times 10^6 = 1220$  and  $1292 \text{ emu/mol}$ , for  $\text{M} = \text{Mo}$  and  $\text{W}$ , respectively). The experimental susceptibilities  $\chi_{\text{DIA}}$  of the diamagnetic silicides  $(\text{TTF})_6(\text{H})\text{SiW}_{12}\text{O}_{40}(\text{Et}_4\text{N})$  (2) and  $(\text{TTF})_6(\text{H})\text{SiMo}_{12}\text{O}_{40}(\text{Et}_4\text{N})$  (4) were very close to the total contribution of the molecules.

After subtraction of the diamagnetic contribution, a paramagnetic temperature-independent term was deduced from a  $\chi_{\text{MT}}$  versus  $T$  plot for the phosphide compounds  $(\text{TTF})_6(\text{H})\text{PW}_{12}\text{O}_{40}(\text{Et}_4\text{N})$  (1) and  $(\text{TTF})_6(\text{H})\text{PMo}_{12}\text{O}_{40}(\text{Et}_4\text{N})$  (3) ( $\chi_{\text{TTF}} \times 10^6 = 1150$  and  $1080 \text{ emu/mol}$ , respectively). Both diamagnetic

and paramagnetic contributions have the same order of magnitude and do not modify the experimental values at low temperature.

**Electronic Band Structure Calculations.** Tight-binding<sup>21</sup> calculations were carried out within the extended Hückel formalism<sup>22</sup> using standard atomic parameters for H, C, S. The exponent ( $\zeta$ ) and the valence shell ionization potential ( $H_{ii}$  in eV) were respectively as follows: 1.3,  $-13.6$  for H 1s; 1.625,  $-21.4$  for C 2s; 1.625,  $-11.4$  for C 2p; 1.817,  $-20.0$  for S 3s; 1.817,  $-13.3$  for S 3p. Calculations were performed on the one-dimensional  $(\text{TTF})_n$  stack running in channels of isolated TTF along the  $c$  direction. X-ray coordinates of salt 3 were used. The symbols  $\Gamma$  and X refer to the points of the Brillouin zone (BZ) of coordinates (0, 0), ( $c^*/2$ , 0), respectively. The  $\Gamma \rightarrow \text{X}$  symmetry line of  $C_{2v}$  symmetry in the reciprocal space corresponds to the  $c$  direction in the real space.

## Results and Discussion

**X-ray Crystal Structures.** All the crystal structures whose stereoscopic view is represented in Figure 1 are built from a polyoxoanion  $\text{XM}_{12}\text{O}_{40}$  unit of  $mmm$  symmetry located at the origin of the C lattice, and three independent TTF molecules (labeled A, B, and C) having  $mm$  or  $2/m$  symmetry (see Table III and Figure 2). The A- and B-type molecules stack regularly with an eclipsed overlap along the [001] direction in channels made of alternating polyanions and TTF molecules of the C-type (see Figures 2 and 3). The disordered  $(\text{C}_2\text{H}_5)_4\text{N}^+$  cations are located on the  $(001/2)$  inversion center.

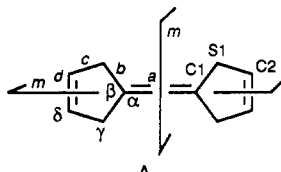
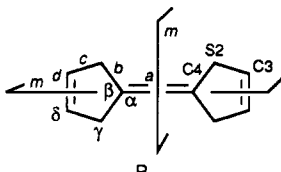
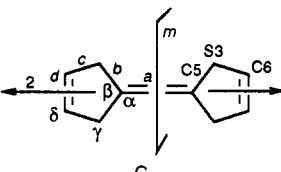
**$\text{XM}_{12}\text{O}_{40}^{n-}$  Units.** The  $\text{XM}_{12}\text{O}_{40}$  units have the  $\alpha$ -Keggin structure.<sup>14</sup> This structure is usually described by the

(20) Frenz, B. A., and Associates Inc. *SDP structure Determination Package*. College Station, Texas, 1985; and Enraf-Nonius, Delft, The Netherlands.

(21) (a) Whangbo, M.-H.; Hoffmann, R. *J. Am. Chem. Soc.* **1978**, *100*, 6093. (b) Whangbo, M.-H.; Hoffmann, R.; Woodward, R. B. *Proc. R. Soc. London, Ser. A* **1979**, *366*, 23.

(22) Hoffmann, R. *J. Chem. Phys.* **1962**, *39*, 1397.

**Table III. Atomic Labeling Scheme of the Constituent TTF Molecules and Their Compared Bond Distances (Å) and Bond Angles (deg) (*mm* and *2/m* Symmetries Are Observed in the Crystal)**

	1, PW <sub>12</sub> O <sub>40</sub>			2, SiW <sub>12</sub> O <sub>40</sub>			3, PMo <sub>12</sub> O <sub>40</sub>			4, SiMo <sub>12</sub> O <sub>40</sub>		
	A	B	C	A	B	C	A	B	C	A	B	C
<i>a</i>	1.31 (3)	1.32 (3)	1.31 (2)	1.32 (4)	1.31 (4)	1.29 (4)	1.33 (2)	1.36 (2)	1.36 (2)	1.37 (3)	1.38 (2)	1.35 (2)
<i>b</i>	1.74 (1)	1.75 (1)	1.76 (1)	1.74 (2)	1.75 (2)	1.77 (2)	1.734 (7)	1.730 (6)	1.751 (7)	1.72 (1)	1.722 (9)	1.758 (9)
<i>c</i>	1.74 (2)	1.76 (2)	1.73 (2)	1.71 (3)	1.80 (3)	1.74 (2)	1.72 (1)	1.727 (9)	1.75 (1)	1.72 (2)	1.72 (1)	1.75 (1)
<i>d</i>	1.30 (2)	1.40 (2)	1.36 (3)	1.28 (3)	1.31 (3)	1.42 (4)	1.34 (2)	1.34 (1)	1.31 (2)	1.42 (3)	1.31 (2)	1.33 (2)
$\alpha$	123.5 (5)	122.9 (5)	123.1 (4)	123.6 (9)	123.2 (7)	123.7 (7)	123.0 (3)	122.5 (3)	122.9 (4)	122.2 (6)	122.2 (5)	123.1 (5)
$\beta$	113 (1)	114 (1)	113.8 (9)	113 (2)	114 (2)	113 (1)	113.9 (7)	115.1 (6)	114.2 (7)	116 (1)	115.5 (8)	113.8 (8)
$\gamma$	96.1 (8)	96.9 (7)	95.9 (8)	95 (1)	96 (1)	98 (1)	96.0 (6)	95.3 (4)	95.3 (4)	96.5 (9)	94.5 (7)	95.6 (7)
$\delta$	117 (1)	116 (1)	117 (1)	118 (2)	117 (2)	116 (2)	117.0 (9)	117.2 (8)	117.6 (8)	116 (1)	118 (1)	117 (1)

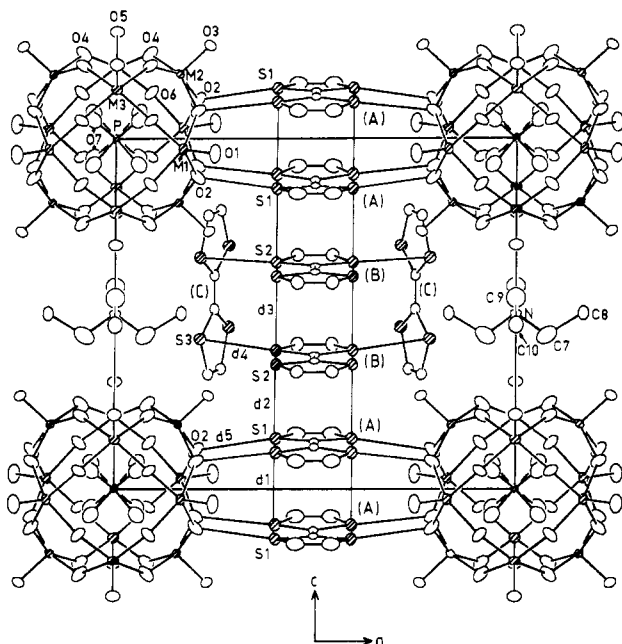


Table IV. Selected Bond Distances (Å) and Bond Angles (deg) for the  $[XM_{12}O_{40}]$  and  $ET_4N^+$  Units

	1 (P, W) <sup>a</sup>	2 (Si, W) <sup>a</sup>	3 (P, Mo) <sup>a</sup>	4 (Si, Mo) <sup>a</sup>
M1-O1	1.66 (1)	1.66 (2)	1.646 (9)	1.63 (1)
M1-O2	1.92 (1)	1.89 (2)	1.939 (7)	1.98 (1)
M1-O6	1.88 (1)	1.89 (2)	1.867 (7)	1.85 (1)
M2-O2	1.85 (1)	1.89 (2)	1.843 (7)	1.831 (9)
M2-O3	1.68 (1)	1.67 (2)	1.649 (9)	1.66 (1)
M2-O4	1.92 (1)	1.93 (2)	1.956 (6)	1.99 (1)
M3-O4	1.88 (1)	1.88 (2)	1.863 (6)	1.85 (1)
M3-O5	1.67 (2)	1.67 (2)	1.665 (9)	1.65 (1)
M3-O6	1.89 (1)	1.89 (2)	1.918 (7)	1.95 (1)
X-O7	1.51 (1)	1.61 (2)	1.531 (9)	1.65 (1)
N-C7	1.48 (5)	1.40 (7)	1.47 (2)	1.52 (4)
N-C9	1.57 (5)	1.58 (8)	1.53 (3)	1.57 (5)
C7-C8	1.64 (6)	1.67 (9)	1.66 (3)	1.62 (4)
C9-C10	1.58 (6)	1.7 (1)	1.62 (3)	1.66 (6)
M1-M2	3.564 (1)	3.534 (1)	3.555 (1)	3.526 (1)
M1-M3	3.565 (1)	3.526 (1)	3.550 (1)	3.525 (1)
M2-M3	3.564 (1)	3.525 (1)	3.559 (1)	3.531 (1)
O1-M1-O2	103.9 (5)	99.8 (7)	100.9 (3)	97.4 (4)
O1-M1-O6	102.9 (5)	102.6 (7)	103.2 (3)	102.4 (4)
O2-M1-O6	86.8 (4)	88.4 (7)	87.1 (3)	88.8 (4)
O6-M1-O6	89.4 (4)	90.4 (6)	92.6 (3)	94.2 (5)
O2-M2-O2	89.8 (4)	90.7 (7)	93.1 (3)	95.7 (4)
O2-M2-O3	100.8 (4)	98.4 (6)	100.2 (3)	98.4 (4)
O2-M2-O4	87.7 (4)	88.9 (8)	87.4 (3)	88.1 (4)
O3-M2-O4	104.6 (5)	103.3 (7)	102.7 (3)	100.2 (5)
O4-M2-O4	83.8 (4)	83.4 (8)	83.1 (3)	82.3 (4)
M1-O6-M3	142.0 (7)	138. (1)	139.4 (4)	135.9 (5)
O4-M3-O5	102.7 (5)	101.3 (8)	102.0 (3)	100.2 (4)
O4-M3-O6	87.8 (5)	89.7 (7)	88.0 (3)	88.5 (4)
O5-M3-O6	102.7 (5)	99.7 (8)	100.2 (3)	97.9 (4)
O6-M3-O6	84.4 (4)	83.7 (7)	83.3 (3)	80.4 (4)
M1-O2-M2	141.9 (5)	138.0 (7)	140.1 (4)	135.3 (5)
M2-O4-M3	139.8 (6)	136 (1)	137.4 (4)	134.0 (6)
O7-X-O7	107.3 (7)	109 (1)	108.4 (5)	106.5 (6)
C7-N-C7	107 (3)	104 (5)	104 (1)	104 (2)
C7-N-C9	110 (1)	114 (2)	110.9 (7)	111 (1)
C9-N-C9	111 (3)	98 (4)	109 (1)	108 (2)
N-C7-C8	111 (3)	111 (6)	109 (1)	107 (3)
N-C9-C10	112 (3)	102 (5)	111 (2)	110 (2)

<sup>a</sup> X, M.

molecule is in the 4f special position and has 2/m symmetry. The atom-numbering scheme, bond distances, and bond angles are given in Table III. From the comparison of the features of the different TTF molecules, it is not possible to distinguish unambiguously the charge borne by each TTF molecule.

The molecules of the A- and B-type form a one-dimensional stack parallel to the [001] direction, with the sequence ...AABBAA... (see Figure 2). All the TTF molecules within the stack are eclipsed (Figure 3). The adjacent TTF molecules of A- or B-type are not related to each other by lattice translations, therefore we observe three intrastack S...S interactions (noted d1, d2, and d3 in Figure 2 and Table V). The small differences between the d1, d2, and d3 spacings suggest a slight tetramerization along the [001] direction with BAAB as a repeat unit. The S...S distances are somewhat shorter than the corresponding van der Waals separations of 3.70 Å and compare well with the corresponding ones observed between eclipsed organic molecules in  $(TTF)_3BF_4$ ,<sup>31</sup>  $(TMTTF)_2Mo_6Cl_{14}$ ,<sup>32</sup> or  $(TMTTF)_2W_6O_{19}$ ,<sup>33</sup> for instance. The environment around

Table V. Selected Intermolecular Interactions (Å) in the  $(TTF)_6[HXM_{12}O_{40}](ET_4N)$  Salts<sup>a</sup>

	1 (P, W) <sup>b</sup>	2 (Si, W) <sup>b</sup>	3 (P, Mo) <sup>b</sup>	4 (Si, Mo) <sup>b</sup>
d1: S1-S1 <sup>i</sup>	3.464 (6)	3.519 (9)	3.484 (4)	3.484 (5)
d2: S1-S2 <sup>ii</sup>	3.566 (6)	3.534 (9)	3.536 (4)	3.540 (5)
d3: S2-S2 <sup>iii</sup>	3.582 (6)	3.567 (9)	3.531 (3)	3.524 (5)
d4: S2-S3 <sup>iv</sup>	3.509 (5)	3.468 (8)	3.476 (3)	3.487 (5)
d5: S1-O2 <sup>v</sup>	3.24 (1)	3.17 (1)	3.131 (7)	3.101 (9)
d6: O3-O3 <sup>vi</sup>	2.60 (2)	2.65 (3)	2.62 (1)	2.69 (2)

<sup>a</sup> Symmetry code: i (x, y, -z); ii (1 - x, -y, z); iii (x, y, 1 - z); iv ( $1/2 - x, 1/2 - y, 1/2 + z$ ); v (1 + x, y, z); vi ( $-1/2 - x, -1/2 - y, 1/2 - z$ ). <sup>b</sup> X, M.

the TTF molecules of type A and B is different since four TTF molecules of type C surround the two B-type TTF of each tetramer perpendicularly to the stack, whereas the two A ones are surrounded by four polyoxoanions (see Figures 2 and 3). Consequently, a different electronic density distribution might result for the TTF molecules of A- and B-type.

**Magnetic and ESR Properties.** If the formula obtained from the X-ray analysis,  $(TTF)_6(XW_{12}O_{40})(Et_4N)$ , is correct, a simple ionic picture  $((TTF)_2^0(TTF)_4^{2+}, (Et_4N)^+(PM_{12}O_{40})^{3-}$  for X = P and  $(TTF)_2^0(TTF)_4^{3+}, (Et_4N)^+(SiM_{12}O_{40})^{4-}$  for X = Si) suggests a diamagnetic behavior for the phosphorus salts and a paramagnetic behavior, due to one unpaired electron on each tetramer of the  $(TTF)_4$  sublattice, for the silicometalate ones.

Surprisingly enough, a temperature-dependent susceptibility was observed below 300 K for the phosphide compounds 1 and 3, after subtraction of the diamagnetic contributions ( $\chi_{DIA}$ ) and the paramagnetic temperature-independent contributions ( $\chi_{TIP}$ ). Figure 4 shows the reciprocal susceptibility for compounds 1 and 3 below room temperature. Anomalies observed around 40 K for compound 1 correspond to a null detection by the SQUID pickup coils due to almost exact compensation between the paramagnetic signal of the sample and the holder diamagnetic contribution.

A Curie behavior was observed over a large range of temperatures, for both compounds. The effective moment  $\mu_{eff}$  deduced from the Curie constants correspond to 1.46 and 1.49  $\mu_B$  for compounds 1 and 3, respectively, characteristic of one unpaired electron. The reciprocal susceptibilities extrapolate to almost zero temperature (see inset in Figure 4) showing that no magnetic interaction is occurring in these compounds.

The effective moment observed for compounds 1 and 3 is due to the presence of one unpaired electron, although somewhat lower than the theoretical value ( $\mu_{theor} = g[S(S + 1)]^{1/2} = 1.73 \mu_B$ , supposing a Landé g factor of 2). A slight reduction of the g factor may partially account for the low effective moment. In fact, related organic donor-inorganic cluster anion systems show also reduced anisotropic g factors, as measured in ESR experiments.<sup>34</sup> In particular, similar magnetic moment values were obtained in the mixed compound  $(TTF)_2(Nb_6Cl_{18})(Et_4N) \cdot (CH_3CN)$  containing  $Nb_6Cl_{18}^{3-}$  units<sup>34b</sup> in  $LuNb_6Cl_{18}^{35}$  or other mixed systems containing  $Nb_6Cl_{12}^{3+}$ .<sup>36</sup> In these latter systems, however, a contamination by diamagnetic  $Nb_6Cl_{12}^{n+}$  (n = 2, 4) units due to off stoichiometry was invoked to explain the magnetic moment of 1.5  $\mu_B$  or less.<sup>36</sup>

(31) Legros, J. P.; Bousseau, M.; Valade, L.; Cassoux, P. *Mol. Cryst. Liq. Cryst.* 1983, 100, 181.

(32) Ouahab, L.; Batail, P.; Perrin, C.; Garrigou-Lagrange, C. *Mater. Res. Bull.* 1986, 51, 1223.

(33) Triki, S.; Ouahab, L.; Grandjean, D.; Fabre, J. M. *Acta Crystallogr.* 1991, C47, 1371.

(34) (a) Penicaud, A.; Batail, P.; Perrin, C.; Coulon, C.; Parkin, S.; Torrance, J. B. *J. Chem. Soc., Chem. Commun.* 1987, 330. (b) Penicaud, A. Thesis, Université de Rennes 1, France, 1988.

(35) Ihmène, S.; Perrin, C.; Peña, O.; Sergent, M. *J. Less Common Met.* 1988, 137, 323.

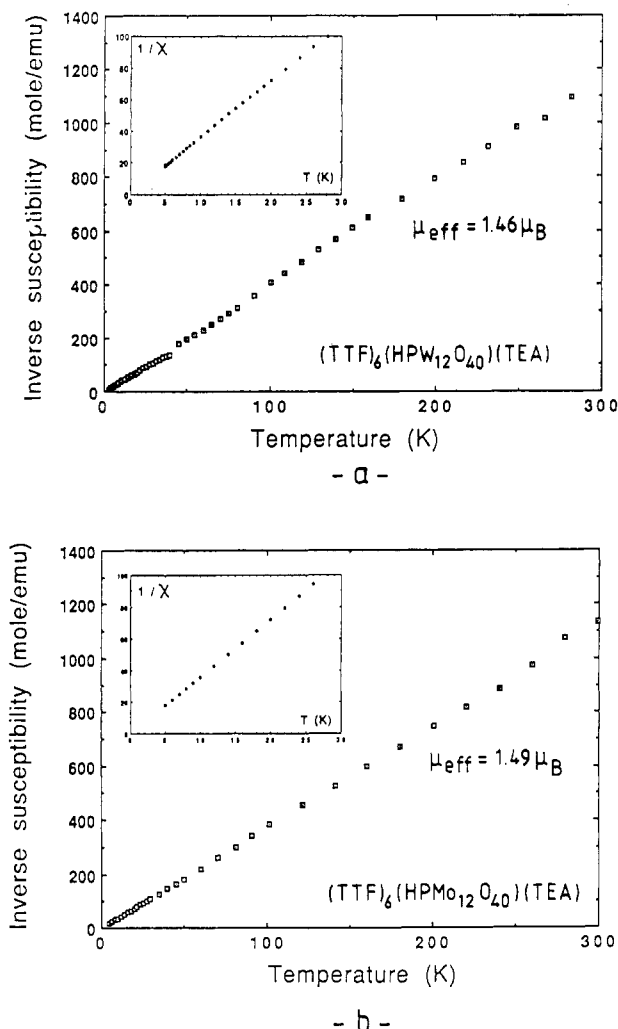


**Figure 4.** Inverse magnetic susceptibility, corrected of diamagnetic and paramagnetic temperature-independent contributions for (a)  $(\text{TTF})_6\text{HPW}_{12}\text{O}_{40}(\text{Et}_4\text{N})$  (1), measured under 10 kOe, and (b)  $(\text{TTF})_6\text{HPMo}_{12}\text{O}_{40}(\text{Et}_4\text{N})$  (3) measured under a 1-kOe magnetic field.

It is also surprising that the silicometalate salts, 2 and 4, exhibit a diamagnetic behavior. Therefore the charge distribution proposed above is questionable and more physical measurements are needed to unravel this point.

Whatever the salt, we did not detect any intrinsic ESR signal at room temperature which could be associated with either the organic or the inorganic sublattice. However, when the different salts were cooled down in liquid helium at 4.2 K, we observed in the case of the phosphometalate salts (1, 3), an ESR signal which broadens and disappears quickly as the temperature increases. On the basis of the 4.2 K spectrum, the  $g$  factor equals 1.826 with a line width equal to 22 G for the compound 1. The corresponding values are 1.947 and 15 G for 3. These values are close to those observed in similar polyanions containing  $\text{W}^{5+}$  and  $\text{Mo}^{5+}$  ( $S = 1/2$ ) species.<sup>37,38</sup> Consequently, we conclude that the phosphometalate anion in 1 and 3 has been re-

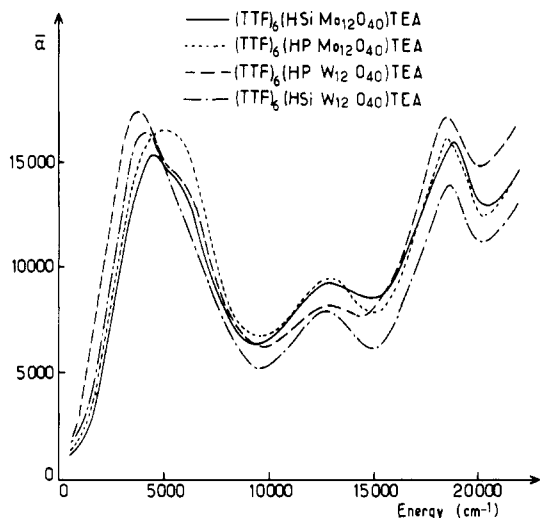


**Figure 5.** Mean electronic absorption coefficient  $\alpha$  versus energy at room temperature.

duced during the reaction process and that the unpaired electron remains localized on a metallic site at low temperature and undergoes a rapid hopping delocalization at room temperature. This is not the case for the silicometalate anion in 2 and 4.

These different results allow us to state that the paramagnetic susceptibility determined from the magnetic measurements carried out on the phosphometalate salts 1 and 3 (see Figure 4) is due to  $\text{W}^{5+}$  and  $\text{Mo}^{5+}$  valence states. Moreover, the existence of only one unpaired electron in the phosphometalate salts 1 and 3 and the absence of any magnetic contribution in the silicometalate salts 2 and 4 lead us to propose a formal oxidation state of 2+ for the TTF tetramers BAAB forming the stack and 0 for the isolated TTF of C-type in every salt. Let us note however that such a statement gives an unbalanced overall charge for the different compounds!

**Electronic and Vibrational Spectra.** The electronic spectra of the four salts shown in Figure 5, indicate the typical charge-transfer bands for conducting salts.<sup>39</sup> Using the Torrance et al. notation,<sup>39</sup> a small band labeled B appears around 13000  $\text{cm}^{-1}$  (1.61 eV) and a relatively strong band labeled A at lower frequency. This peak A, characteristic of a mixed-valence state, is broad and presents a shoulder on the blue side. Its maximum is around 3700  $\text{cm}^{-1}$  (0.46 eV) for the tungsten salts, around 4500–5000  $\text{cm}^{-1}$  (0.56–0.62 eV) for the molybdenum ones. Therefore, we note an apparent influence of the anion-cation interactions on the charge-transfer energy which is due to the change of the metal atom (W or Mo) of the anionic clusters, in spite of a similar electronegativity value in Pauling's scale and identical ionic radii of W and Mo.

Variable-temperature infrared absorption spectra from 15 to 300 K were recorded for the four samples. One of them, the spectrum obtained for the silicotungstate compound 4, is given in Figure 6. Beyond the tail of the electronic band A, we observe the vibronic band  $\nu(\text{C}=\text{C})$  around 1350  $\text{cm}^{-1}$  (0.17 eV) resulting from electronic-molecular vibration (e-mv) coupling as in previous TTF salts,<sup>40</sup> and other intense bands below 1000  $\text{cm}^{-1}$  due to the polyoxoanion.<sup>41</sup>

(36) Converse, J. G.; Mc Carley, R. E. *Inorg. Chem.* 1970, 9, 1361. Mackay, R.; Schneider, R. *Inorg. Chem.* 1967, 6, 549.

(37) Varga, G., Jr.; Papaconstantinou, E.; Pope, M. T. *Inorg. Chem.* 1970, 9, 662.

(38) (a) Prados, R. A.; Pope, M. T. *Inorg. Chem.* 1976, 15, 2547. (b) Sanchez, C.; Livage, J.; Launay, J. P.; Fournier, M.; Jeannin, Y. *J. Am. Chem. Soc.* 1982, 104, 3194.

(39) Torrance, J. B.; Scott, B. A.; Walter, B.; Kaufman, F. B.; Seiden, P. E. *Phys. Rev.* 1979, B19, 730.

(40) (a) Bozio, R.; Zanon, I.; Girlando, A.; Pecile, C. *J. Chem. Phys.* 1979, 71, 2282. (b) Bozio, R.; Pecile, C. *J. Phys. C, Solid State Phys.* 1980, 13, 6205.



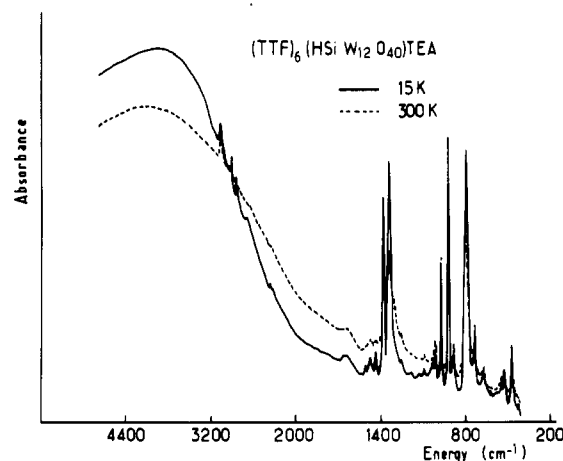


**Figure 6.** IR absorption spectra (arbitrary units) between 4800 and 360  $\text{cm}^{-1}$  of  $\text{TTF}_6\text{HSiW}_{12}\text{O}_{40}\text{Et}_4\text{N}$  at 300 K (---) and at 15 K (—).

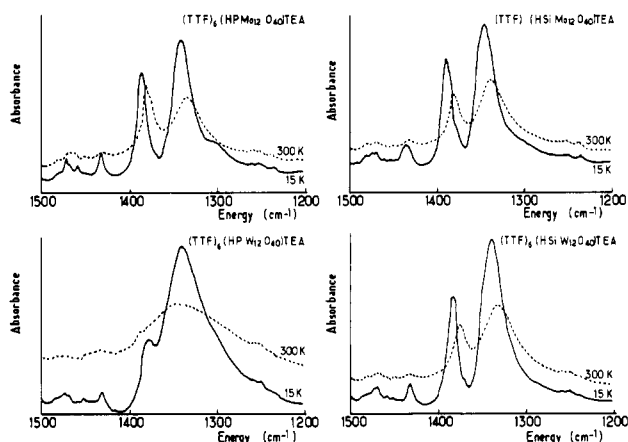


**Figure 7.** IR absorption spectra (arbitrary units) between 1500 and 1200  $\text{cm}^{-1}$  at 300 K (---) and at 15 K (—) of  $\text{TTF}_6\text{HPW}_{12}\text{O}_{40}\text{Et}_4\text{N}$ ,  $\text{TTF}_6\text{HSiW}_{12}\text{O}_{40}\text{Et}_4\text{N}$ ,  $\text{TTF}_6\text{HPMo}_{12}\text{O}_{40}\text{Et}_4\text{N}$ , and  $\text{TTF}_6\text{HSiMo}_{12}\text{O}_{40}\text{Et}_4\text{N}$ .

The representative part (between 1500 and 1200  $\text{cm}^{-1}$ ) of the infrared vibrational spectra is enlarged and shown in Figure 7 for the four salts at 15 K (solid line) and 300 K (dashed line). Compared to the three others, the phosphotungstate salt 3 behaves differently. Between 1450 and 1300  $\text{cm}^{-1}$ , the spectrum of 3 (recorded for several samples), presents always only one strong and broad band around 1340  $\text{cm}^{-1}$  at room temperature. This band narrows and shifts to higher energy as the temperature decreases. At low temperature, we also observe a small peak around 1380  $\text{cm}^{-1}$ .

In the three other spectra shown in Figure 7, two well-resolved and strong peaks are seen at 1380 and 1340  $\text{cm}^{-1}$ , at any temperature the more highly energetical one being less intense than the other; their frequencies decrease slowly with the temperature. Therefore, no structural phase transition has been detected for any of the four salts in the full range of temperature.

Let us note that the IR-active modes of neutral TTF are not observed because the charge-transfer band and associated vibronic modes are very intense and prevent their detection. It results therefore that the two vibronic modes

are attributed to the mixed-valence system formed by the A- and B-type TTF of the stack. The presence of two bands instead of one might be due to the fact that the A- and B-type TTF forming the tetramers BAAB of the organic stack in the four compounds are nonequivalent. Several years ago, Yartsev proposed a model<sup>42a</sup> showing that for quasi-isolated tetramers bearing two electrons (...BAABBAAB...), two IR and two Raman modes are expected for a given vibration if molecules A and B do not bear the same electronic charge. More recently, this model has been extended to superclusters where the neighboring tetramers are in the interaction.<sup>42b</sup> Indeed the frequencies of the Raman bands are related to the charge of the molecules and are proportional to the mean charge borne by the TTF molecules.<sup>43</sup> The two IR bands, i.e., the  $A_g$  modes activated by the e-mv coupling, present a frequency difference greater than the one which would be observed in Raman. In the present case, we observe a difference of about 40  $\text{cm}^{-1}$  between the two peaks which might mean that there is a significant difference between the A and B sites. From Raman scattering experiments<sup>43</sup> we can estimate only the mean charge difference ( $\Delta\rho < 0.4$ ) between the two kinds of TTF molecules. But, in absence of Raman data, we are not able to estimate the e-mv coupling constants and consequently the absolute charges on the A and B TTF molecules.

Indeed, the A- and B-type TTF molecules are electronically different (vide infra) and the band A and its shoulder observed in all the spectra shown in Figure 5 can be assigned to the two electronic bands which are expected for the tetramer BAAB. The transfer integrals  $t$  and  $t'$  between the neighboring molecules B-B and B-A, and A-A, respectively, are in the same order of magnitude. Their ratio is estimated  $t'/t = 1.1$ , a case not explicitly examined by Yartsev et al.<sup>42</sup> but which might be similar to those presented ( $t'/t < 1$ ).

**Electronic Band Structure.** The different results obtained for the title salts lead us to draw some conclusions. First, no direct structural interaction seems to occur between the organic and inorganic parts. Second, assuming from structural and spectroscopic properties that for every salt a total charge of 2+ is distributed over the organic  $\text{TTF}_6$  sublattice, we can think that  $(\text{TTF}_4)^{2+}$  chains (A- and B-type TTF molecules) run along channels made of isolated and neutral TTF (C-type TTF molecule, see Figures 2 and 3). The question which arises from the previous section is the following: is the 2+ charge equally distributed over the TTF molecules A and B forming the tetramers of the  $(\text{TTF}_4)^{2+}$  stack?

To test this statement, we performed extended Hückel tight-binding band calculations on the "isolated" one-dimensional chain of  $(\text{TTF}_4)^{2+}$ . A slight but noticeable charge difference of 8% is computed between the A- and B-type TTF molecules of each tetramer BAAB. The charge of A is +0.52 whereas that of B is +0.48. This is in agreement with the results proposed above. The difference is tiny since the *intertetramer* spacing ( $d_3$  between B and B) is close to the *intratetramer* spacing ( $d_1$  between A and B, and  $d_2$  between A and A; see Figure 2 and Table V).

Band calculations were also carried out on the one-dimensional chain of  $(\text{TTF}_4)^{2+}$  surrounded by the isolated

(41) Rocchioli-Deltcheff, C.; Thouvenot, R.; Franck, R. *Spectrochim. Acta* 1976, 32A, 587.

(42) (a) Yartsev, V. M. *Phys. Status Solidi* 1984, B126, 501. (b) Yartsev, V. M.; Swietlik, R. *Rev. Solid State Sci.* 1990, 4 (1), 69.

(43) Matsuzaki, S.; Moriyama, T.; Toyoda, K. *Solid State Commun.* 1980, 34, 857.



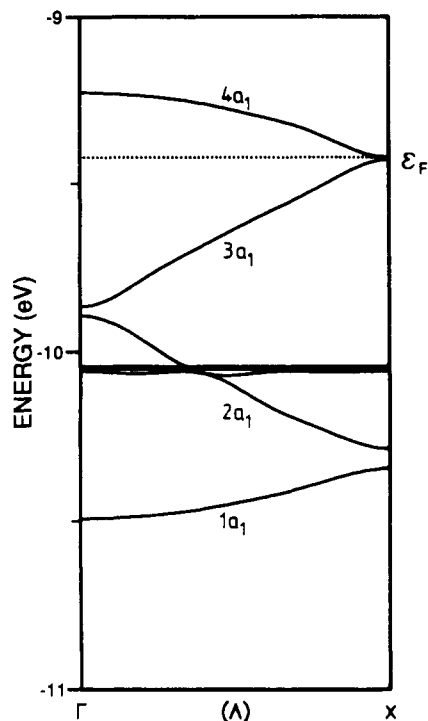


**Figure 8.** Dispersion relations of the bands deriving from the HOMO of the TTF molecules constituting the organic chains of the polyoxoanion salts. The unit cell of the one-dimensional chain is made of two A-type and two B-type TTF molecules plus four perpendicular C-type TTF molecules surrounding the B-type ones.

C-type TTF molecules in order to measure the interaction of the latter with the B molecules of the stack. The dispersion relations of the eight bands deriving from the HOMO of the eight TTF molecules contained in the unit cell are shown in Figure 8. Slightly below  $-10.0$  eV, we note the presence of a bunch of four bands completely flat all along the  $\Gamma \rightarrow X$  symmetry line. The flatness of those bands, almost exclusively localized on the four C-type TTF molecules present in the unit cell, means that they are isolated from each other and from the  $\text{TTF}_4$  chain. They lie largely below the Fermi level and consequently are occupied, reflecting their neutral character. No electron transfer toward the  $\text{TTF}_4$  chain is noted despite some rather short nonbonding  $\text{S} \cdots \text{S}$  contacts (see *d4* in Figure 2).

The four other bands of  $a_1$  symmetry shown in Figure 8 concern the four TTF molecules of the unit cell stacking along the  $c$  direction. They are rather more dispersive.  $\sigma$ -type interaction, mainly through S atoms, occurs between the eclipsed TTF molecules constituting the chain running along the  $c$  direction. The small bandgaps observed between  $3a_1$  and  $2a_1$  bands at  $\Gamma$  and between  $1a_1$  and  $2a_1$  and between  $3a_1$  and  $4a_1$  at X suggest that a very weak tetramerization has occurred in the  $\text{TTF}_4$  chain. This Peierls-like distortion was expected somewhat since with a formal oxidation of  $2+$  for  $\text{TTF}_4$ , a three-quarter-filled band is obtained before distortion. After distortion a very small bandgap of less than  $0.01$  eV is computed between the valence and the conduction bands. Some poor conductivity is expected along the organic chains in our salts as observed experimentally (*vide supra*).

While a neutral charge is observed for the isolated C-type TTF molecules, a charge of  $\text{ca. } +1/2$  is calculated for each A- and B-type TTF molecules of the chains. This charge assignment is in agreement with the fact that at  $\Gamma$  the energy of the band derived from the HOMO of the

neutral C-type TTF is slightly below than that of the nonbonding  $2a_1$  and  $3a_1$  bands which come from the HOMO of the positively charged A- and B-type TTF. Indeed the energy of the HOMO level of TTF which is strongly bonding between the central C atoms<sup>44</sup> is expected to increase with the positive charge of TTF. This results in the so-called intramolecular relaxation.<sup>45</sup>

Finally let us remark that the bands relative to the  $(\text{TTF}_4)^{2+}$  chains are sufficiently wide to prevent any electron localization which would render the chains magnetic. Therefore a low-spin occupation is likely to occur in agreement with the ESR data (*vide supra*).

### Conclusion

The main results which come out from this study are the following:

(i) The reaction of the tetrathiafulvalene with the tetraethylammonium salt of Keggin polyoxoanions is possible and leads to the formation of a new and interesting type of charge transfer salts.

(ii) According to both static and dynamic magnetic data, the obtained silicometalate salts 2 and 4 are diamagnetic while the phosphometalate salts 1 and 3 are paramagnetic with only one unpaired electron localized on the inorganic anion cage. Low-temperature ESR measurements indicate that this unpaired electron, trapped during the reaction process, is localized on one metallic site. Therefore both silico- and phosphometalate anions bear the same charge of  $4-$  in the synthesized salts 1–4.

(iii) Optical properties and band structure calculations demonstrate the presence in these different salts of neutral and isolated C-type TTF molecules and stacks of tetramers bearing two positive charges slightly not uniformly distributed on the A- and B-type TTF molecules.

With these different results, a point remains to be unravelled: the global charge distribution. Indeed, for every salt a negative charge of  $4-$  per polyoxoanion is observed whereas a positive charge of only  $3+$  is obtained for the organic part ( $2+$  due to the TTF sublattice and  $1+$  due to the  $\text{Et}_4\text{N}^+$  cation). The first idea coming to mind is that a proton has been trapped around the inorganic cages during the synthesis of the salts 1–4. This is common in the chemistry of polyoxometalates.<sup>6,10</sup> Therefore, to equilibrate the negative and positive charges, we propose that the appropriate formula for all of the title salts is  $(\text{TTF}_2)^0(\text{TTF}_4)^{2+}(\text{H})^+(\text{Et}_4\text{N})^+(\text{XM}_{12}\text{O}_{40})^{4-}$ . Such a charge distribution particularly accounts for the paramagnetic behavior of the phosphometalate salts (1 and 3) and the diamagnetic properties of the silicometalate ones (2 and 4). To confirm this statement, a NMR study of these salts would be needed. We have indeed synthesized quaternary salts in which it will be possible to vary the different counterions for modulating the physical properties.

**Acknowledgment.** We thank Pr. M. T. Pope, Pr. J.-Y. Saillard, and Pr. V. M. Yartsev for helpful comments and L. Hubert for the drawings.

**Registry No.** 1, 140201-90-7; 2, 140201-92-9; 3, 140201-94-1; 4, 140201-96-3.

**Supplementary Material Available:** Tables of atomic coordinates, bond distances, bond angles, and thermal parameters (12 pages); tables of calculated and observed structure factors (30 pages). Ordering information is given on any current masthead page.

(44) Lowe, J. P. *J. Am. Chem. Soc.* **1980**, *102*, 1262.

(45) Shaik, S. S.; Whangbo, M.-H. *Inorg. Chem.* **1986**, *25*, 1201.